ISSN 2447-6102

Article

Measurements of convective heat transfer around a single rod bundle for three gap spacing

Kayser, F.M. [1,]*, Ferrari, J.M.S. [2] and Goulart, J.N.V. [3]

[1] Group of Experimental and Computational Mechanics — GMEC, University of Brasilia; fabio_mk_66@hotmail.com
[2] Group of Experimental and Computational Mechanics — GMEC, University of Brasilia; jalusaferrari@gmail.com
[3] Group of Experimental and Computational Mechanics — GMEC, University of Brasilia; jvaz@unb.br

* Correspondence: fabio_mk_66@hotmail.com

Received: 06/11/2020; Accepted: 05/12/20; Published: 31/12/2020

Abstract: This work aims to evaluate the experimentally the convective heat transfer coefficient around a single rod bundle under turbulent flow. The single rod bundle is part of a compound channel that is mainly characterized by their dimensionless numbers such as the Reynolds number, and the *W/D* - ratio. The gap width, *δ,* is the distance between the rod and the upper part of the channel. During the experimental campaign, the gap *δ* was changed its width to 5, 10 and 15 mm, yielding a *W/D* = 1.05, 1.10 and 1.15, respectively. The dimension *W* is the sum of the gap width, *δ*, and the cylinder's diameter. The test section length was kept constant, 1800 *mm*. Special heated cell, controlled by a Minipa 3305 Power Supply, was designed in order to keep cell`s surface heated. The temperature on the cell`s surface was acquired through a set of special thermocouples on it. Afterwards, the wall temperature and the local minima in terms of convective heat transfer coefficient around the tube was determine and compared with those ones from the open literature. The J-data were found in fair agreement with those previously published. Moreover, the J-data location was not found in the narrow gap for the smallest W/D studied, but for locations away the gap (0°). When the gap becomes wider, the lowest local $\overline{h}$ returned to the narrow gap position. Hot-wire probe was employed to measure the mean average and the turbulent velocity time traces at the gap vicinity. Coherent structures were seen to dominate the flow at such region, affecting the J-data locus.

Keywords: Nusselt number, Heated cell, Compound channel, Rod bundle, Coherent structures.

1. Introduction

Channels with a main channel containing subchannels connected by gaps are known as compound channels (Ferrari and Goulart, 2015; Goulart et al., 2016 and Melo et al., 2017). Flow in structures with compound channels are characterized by instabilities and values of the turbulent stresses that are not found in another simple channel (Goulart et al., 2016; Severino, 2018; Candela et al., 2020).

Convection is a heat transfer mechanism that involves both heat transfer by conduction and by advection (fluid movement). When studying convection, it is common to use equations in the dimensionless form, that allow us to reduce the number of variables we must deal with. In this respect, it ends up dimensioning the convection heat transfer coefficient (h) in form of the Nusselt Number.

The heat transfer process and the mean average flow in closely-spaced rods have been extensively studied over the 5 or 6 decades, at least (Palmer and Swanson, 1961, Groenveld, 1973, Ouma and Tavoularis, 1991, Guellouz and Tavoularis, 1992, Makhmalbaf, 2012). To raise awareness on the knowledge of the convective heat coefficient, h, its distribution around the tubes and its dependence on the type of rod arrangement, is prime to ensure both the operational safety and the performance of the thermal devices as heat exchangers and nuclear reactors.

This work aims to evaluate experimentally the convective heat transfer processes in a closed compound channel. The experimental campaign was carried out in a rectangular channel containing a single rod inside for 3 different W/D

– ratio, 1.05, 1.10 and 1.15. Part of the rod is heated by a special device developed in our laboratory, and the temperature is controlled by a power supply. The rod heated part was able to turn around its own axis, that enable us to gather the average local wall temperature and, therefore, the local convective heat transfer around the tube. During the experimental campaign, the temperature field was measured on the tube's wall, and for the three cases, as well as, the mean average Nusselt number, its variation and the local one. We also calculates de J-data, based on lowest local value of the convective heat transfer coefficient, h. Despite of our expectations the locus of the lowest local convective heat transfer is not in the narrow gap, but instead, nearby. To evaluate the dynamic of the flow single hot wire probe was employed. Velocity fluctuations were gathered throughout the experiments showing energetic peaks in the spectra for all three gap spaces (1.05; 1.10 and 1.15).

The experiment was performed under the Reynolds condition, Re_{Dh} = 42000, based on the bulk velocity, U_{Bulk}, the hydraulic-diameter, D_h and the kinematic viscosity, ν. Air, at room temperature, was used as a work fluid, yielding a Prandlt number about 0.7.

2. Experimental procedure

The experiment was carried out in an acrylic rectangular aerodynamic wind channel, whose air, at room temperature, is insufflated a centrifugal fan at the extremity, according to Figure 1. After passing by a set of screens and honeycombs the free stream velocity, Uref is measured by a fixed Pitot tube. The mass flow rate is controlled by a frequency inverter connected to the fan.

The teste section is formed by a single rod bundle apart from the channel`s upper wall by a distance d. In this way both lateral subchannels are connected through the thigh gap.

Figure 1 (a) and (b) shows the lateral view and the transversal section of the channel. The total length of the channel (LT) is 3000 mm, the test section length (LS) is 1800 mm. The dimensions L1 and L2 are 525 mm and 475 mm, respectively. For the transversal section, WC = 200 mm, HC = 150 mm and D = 100 mm. In this experiment were used three gap width (d), 5, 10 and 15 mm.

The velocity and spectra were gathered by the hot-wire technique. The data processing was carried out in the TSI IFA-300 hot-wire system. The TermalPRO software, available by the manufacturer, conducted the calibration and the data gathering. It was used a single probe TSI 1201 to gather the velocity time-traces. The velocity signals were sampled at 1 kHz with a low pass filter set at 300 Hz, and digitalized by a A/D board 16 Bits.

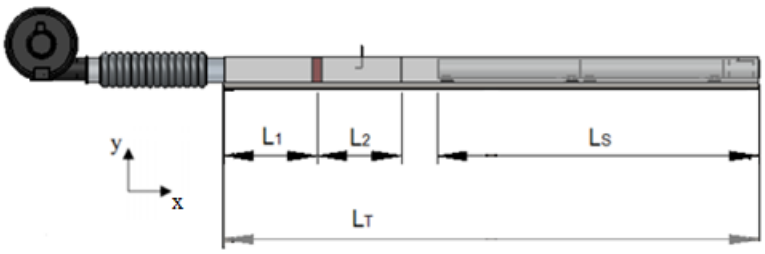

(**a**)

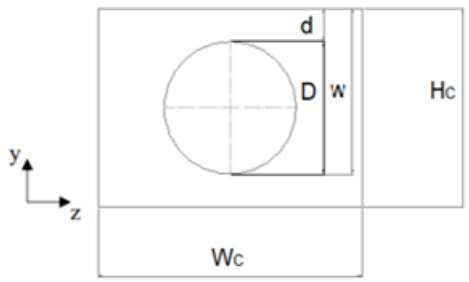

(**b**)

Figure 1. Channel's dimensions. (**a**) Lateral view; (**b**) Transversal section.

At the end of the rod, about 200 *mm* upstream the channel`s outlet there is a heated cell mounted on the of the rod, as shown in Figure 2. The cell is heated by a MINIPA MPL-3305M electrical source and is completely insulated. The cell can be turned around the axis's rod, assuming different angular position. In order to acquire the

temperatures, five thermocouples were placed in the heated cell and in the adjacent region. According to the indications seen in the Figure 2, the thermocouples were place in the surface of the heated cell (*S*), in front (*F*), in the right side (*RS*), in the left side (*LS*) and allow the heated cell (*I*), in the inner part of the tube. In the surface of the heated cell was used an Ômega SA1XL-T-72 thermocouple and in the other points was used a 5TC-GG-K-20-72 thermocouple. The thermocouples were connected to a Novus FieldLogger module, which is responsible for transferring the temperature data to a computer through a USB cable.

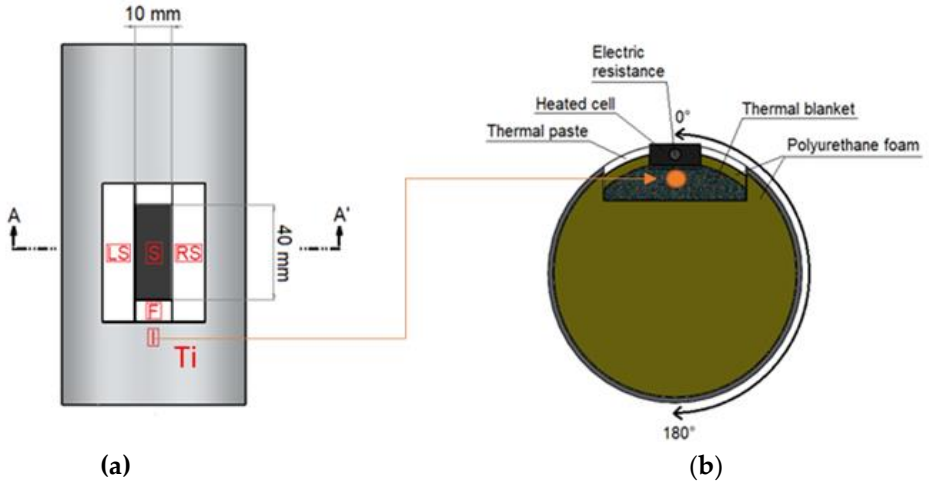

Figure 2. Heated cell. (**a**) Superior view; (**b**) Cross section.

The heated source was figure out as a cartridge resistance housed by an aluminum metal piece. The electrical source Minipa was responsible feeding such resistance at a determined voltage and current (V and I), that remained constant throughout the experiment. The heated cell was powered by the electrical source with q_f = 1 W. In order to find the convective heat transfer coefficient, first, was necessary to make some considerations about the heat distribution near the heated cell. As said before different thermocouples were distributed in different regions of the heated cell. First, the heated cell was turn on for no-flow condition, in order to observe the how the temperatures rises at different location of the heated cell. Such observation lasted, for at least hours. After this time was observed that the temperature on the small plate (thermocouple S), raised up from the room temperature up to 65 °C. In a meanwhile, four other thermocouples were observed. The lateral and frontal thermocouples (F, LS and RS) were seen to change its temperature only 2 degrees in regards to the room temperature, whereas the lower thermocouple (I) showed temperature values up to 6 °C beyond the room temperature.

Due to this, it has been established that the heat transfer was nearly one-dimensional. Assuming that the electric power is entirely converted into thermal energy by the cartridge resistance and the thermal flow energy transferred to the main, q_{conv}, flow is the major, but not the entire part of the thermal power, q_f, we can write

$$q_{conv} = q_f - q_L \tag{1}$$

Where q_L is the thermal power lost due to the conduction mechanism.

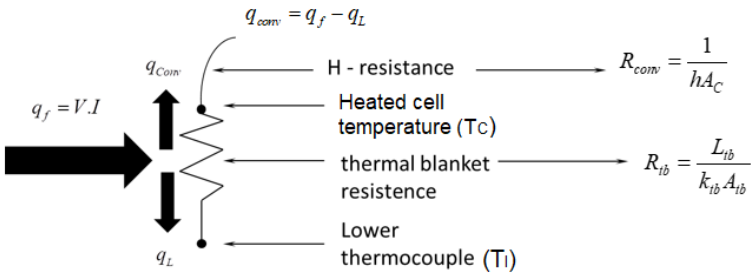

Figure 3. Model for compute the heat loss.

The conduction heat process between the cell and the thermal blank is (q_L), and is given by,

$$q_L = \frac{T_C - T_I}{R_{tb}} \tag{2}$$

R_{tb} is the thermal resistance between the thermal blanket and the heated cell, k_{tb} = 0.04 w/mk is the thermal conductivity of the thermal blank, A_{tb} = 0.00165 m², TC is the heated cell temperature, T_I is the thermal blank surface temperature and L_{tb} = 15 mm is the thermal blank thickness.

On the other hand, R_{conv} is the thermal resistance between the heated cell and the air flow. The convective heat transfer was then calculated as,

$$q_{conv} = \frac{T_\phi - T_\infty}{R_{conv}}$$
$$R_{conv} = \frac{1}{h_\infty A_C} \tag{3}$$

In the set of Equation (3) T_ϕ, T∞ and h∞, AC , are the mean average temperature at each angular position around the cylinder, the mean average flow temperature inside the channel and the calculated heat transfer coefficient at each angular position and the plate's area (0.0004 m), respectively. After rescaling the convective heat transfer (q_{conv}), it is possible to re-write the convective heat transfer coefficient in terms of Nusselt number, based on the hydraulic-diameter and the air thermal conductivity, k_{air}. Afterwards, Nusselt numbers at each azimuthal position, Nu_Φ, were scaled by using the average Nusselt number, $\overline{Nu\phi}$, as follow in Equation (4), producing an spatial Nusselt number variation, ΔNu_Φ

$$Nu_\phi = \frac{\bar{h}_{(\phi)} D_h}{k_{air}}$$
$$\Delta Nu_\phi = \frac{Nu_\phi}{\overline{Nu_\phi}} \tag{4}$$

3. Results

3.1. Temperature, h and Nusselt distribution around the rod

Figure 4 (a) shows the dimensionless temperature distribution around the rod, being 0° the narrow gap position and 180° the wider gap. The temperature is re-scaled by using the mean average flow temperature, T_∞ (which is almost the inlet temperature) and the wall temperature as function of the angular position,

$$T_\phi = \frac{\overline{T_{w(\phi)}} - \overline{T_\infty}}{\overline{T_{w(\phi)}}} \tag{5}$$

Before starting the measurements the facility was turned on for time enough in order to reach the stationary condition for each angular position, so, the mean flow average temperature, $\overline{T\infty}$ for each W/D case was 36.77°C, 36.24°C and 36.84°C (1.05, 1.10 and 1.15, respectively).

From the Figure 4 (a) is possible to see that the temperature is higher at the narrow gap vicinity and decreases as the angular position is further changed towards 80°. At this point the temperature reaches its minimal, where the local h(ϕ) is the highest, as seen in Figure 4 (a and b). With regards the Nusselt number variation, its distribution is present some peak at the maim subchannel where we expected higher axial velocities. Despite the gap space the highest variation of the Nusselt number was about ΔNu_ϕ ~ 0.1, taking place at the same region. Further, the distribution of variation of the Nusselt number ΔNu_ϕ is in completely agreement with the computations carried out by Chang and Tavoularis, 2007 and 2008, in spite of the Reynolds number difference.

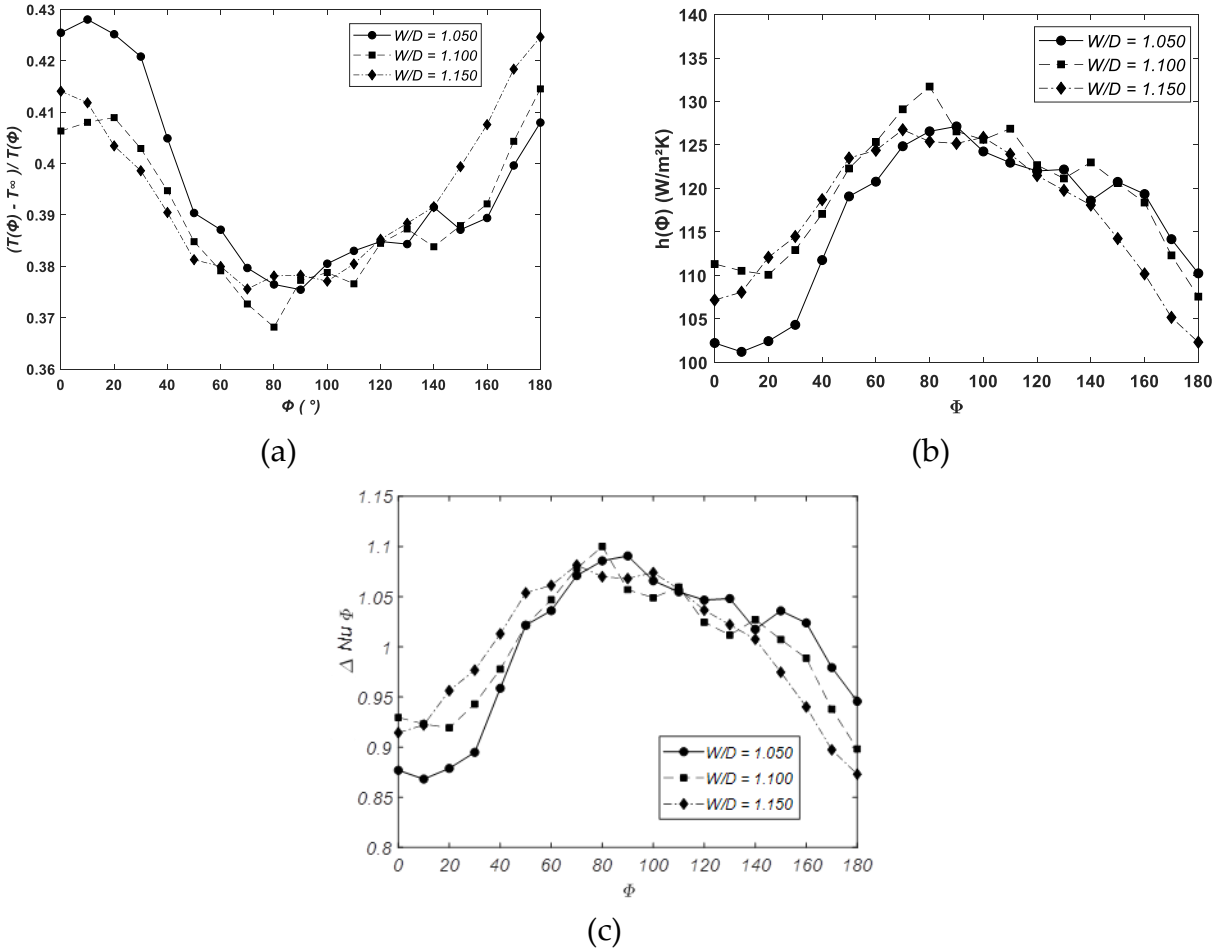

Figure 4. (a) Temperature and (b) $\overline{h}_{\phi}$ distribution around the rod from 0° to 180° (c) Nusselt number distribution around the tube.

In this paper, we are very interested in determining both the lowest and highest $\overline{h}_{(\phi)}$ locus, since such information is prime to understand the connection between the main flow and the convective heat transfer coefficient. Taking a careful look at the first angular positions of the Figure 4 (a) it is possible to see that the temperature does not present the same behavior, despite the fact that the temperature is higher at these positions for any W/D-ratio studied. As the narrow gap become wider the local Reynolds number also increases (Groeneveld, 1973, Chang and Tavoularis, 2008), promoting an improvement in terms of heat transfer, and therefore increasing the mean average convective transfer. Afterwards, the local and mean average convective heat transfer coefficient is easy to compute, as shown in Figure 4 (b).

As said before as the narrow gap becomes narrower the local Reynolds number becomes less important and the heat is transferred poorly. In fact, $h_{\phi}/\overline{h}$ (or ΔNu_{ϕ}, since they are scaled using the same variables) reaches its smallest value for the narrowest gap, W/D = 1.05. For the next W/D- ratio, 1.10 and 1.15, the ratio $h_{\phi}/\overline{h}$ are almost the same, but an inversion in their values was seen, producing a kind of flaw in our expectations. However, such result can be explained by observing the flow velocity fluctuation, that will discussed in the next item.

Many researchers have being conducting thermal measurements in rod bundles over the years. One of the purposes is to identify and quantify the locus of the lowest ratio $h_{\phi}/\overline{h}$ that has been called J-data. Groeneveld (1973), Guellouz and Tavoularis (1992) and Guellouz (1998), in his PhD thesis stressed a number of researchers who quantified such value, including, producing equations whose the gap spacing W/D – 1, was the variable. Such equations neither observed the rod position nor the bundle arrangement.

Present J-data is shown in Figure 5, along with the data from Guellouz (1992) (whose values are better stressed in his PhD thesis) and the fit proposed by Groeneveld (1973). From the Figure 5, we can see that the J-data measured in the present work and those from Guellouz and Tavoularis (1992), are in fair agreement. Further, as the

W/D increases the J-data becomes the unity. Such behavior is completely expected, since the $h_\phi / \overline{h}$ is thought to be almost constant for higher W/D-ratio, see the concentric pipe flow at the same conditions.

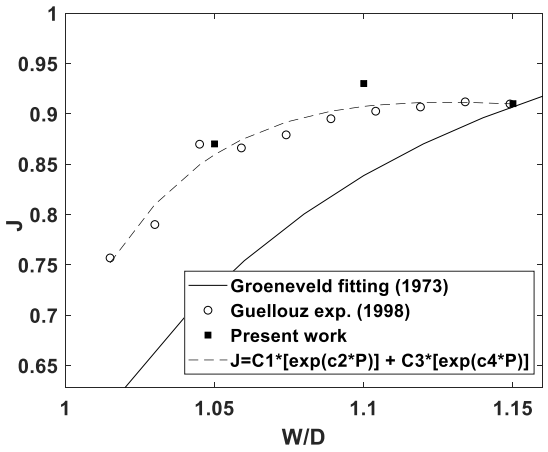

Figure 5 – J-data as a function of W/D-ratio.

For the proposal equation to fit both data (present work and that one from Guellouz and Tavoularis, 1992), c1 = 0.9788; c2 = -0.4137; c3 = -0.3108 and c4 is -22.78, P is the gap space, W/D – 1.

3.2. The flow dynamics

Over the last 60 years a lot of studies have being aimed to measure and understand the dynamics of either the laminar or turbulent flows in channels whose the main characteristics is to be compound (Hoffmam, 1964, Rowe et al., 1973, Hopper and Rehme, 1984, Möller, 1991, Meyer and Rehme, 1994, 1995, Severino et al., 2018, Candela et al., 2020, among others). These works were conducted in a different channel, using different methodologies and shapes, however, the channels, always, were characterized by a narrow gap connecting one or more subchannels. The spectral response of the velocity time-traces gathered in such channels showed difference response in comparison with that expected from Kolmogorov theory, instead, high peaks in the spectra were seen indicating the large coherent structures presence dominating the gap vicinity. Such structures were seen, for far, as the main responsible for increasing the mixing rate between two adjacent subchannels (Meyer, 2010), since they promote the crossing flow between subchannel. The main mechanism behind such mixing is that the poor thermal flow in a subchannel is carried to another adjacent one through the tight gap, giving rise to a crossing flow.

Taking this into account we carried out velocity time-traces measurements for each W/D- ratio studied. Hot-wire probe was running from the narrow gap middle plane up to z = r. As regards the y-direction the probe was moved from 40° up to 0°. Figure 6 (c) shows the area where the velocity time-traces were gathered. Our previous results indicated that the coherent structures were not identified by the probes neither for distances much further away from the gap nor for azimuthal positions further form 30°, in this sense we delimited an area as the reader can see below.

In this section the dimensionless velocity spectrum will be presented. This analysis shows the presence of the large-scale structures in the flow, through the presence periodic pattern in the velocity time-traces. The frequency was dimensionless by the Strouhal number. The Strouhal number was determined by the Equation (6), using the bulk velocity, Ub, the tube diameter, Chang and Tavoularis (2007 and 2008), calculated the Strouhal number the same way. According to the authors, using the tube diameter to find the Strouhal number is more appropriate, because the hydraulic diameter is mostly determined from parts away from the gap. The spectrum energy was dimensionless by using as scales the bulk velocity and the tube's diameter, according Equation (7). The bandwidth of the spectra is 0.97 Hz.

$$St = \frac{fD}{U_b} \tag{6}$$

$$\psi = \frac{\overline{u'^2}}{DU_b Hz} \tag{7}$$

The velocity time-traces were measured in the line of the 0° position in the gap. For W/D = 1.05 spectra was gathered 25 mm away from the center of the gap, whereas, the other two W/D-ratio (1.10 and 1.15), data sample measured 30 mm away from the center of the gap

Figure 6 shows the dimensionless spectra of the fluctuating axial velocities for W/D = 1.05, 1.10 and 1.15. In any of the spectra, sharp peaks can be seen. It means that the energy of the fluctuations are mainly contained at some frequency (or Strouhal) bandwidth, besides the fact that the flow field stresses periodical patterns, indicating the large scale structures at the gap vicinity.

The main frequency in the spectra and Strouhal numbers for the W/D = 1.10 and W/D = 1.15 are almost identical, being at St = 0.43, for both gaps size. Actually, a marginal difference was realized, but is inside our uncertain in terms of frequency. On the other hand, the for the gap size 5 mm (W/D = 1.05), lower Strouhal number was found, St = 0.33.

Despite de values encountered our dynamic low response are from that presented by Guellouz and Tavoularis (2000) and Severino *et al.* (2018) who found Strouhal numbers about 0.20 in a very similar channel. However, it noteworthy to mention that the measurements carried out by Severino *et al.* (2018) showed a certain data scattering in terms of Strouhal number, whose values were seen to vary from 0.29 up to 0.15.

Another source of explanation lies in the fact that both authors (Guellouz and Tavoularis, 2000 and Severino, 2018) carried out their experiments using a hollow test section, whereas the test section used in this work has both sides closed. It might be an explanation for the discrepancy in the Strouhal number, since the local velocity distribution might be affects the dynamic of the large vortices in the gap. A further experimental campaign must be carried out to devise an explanation.

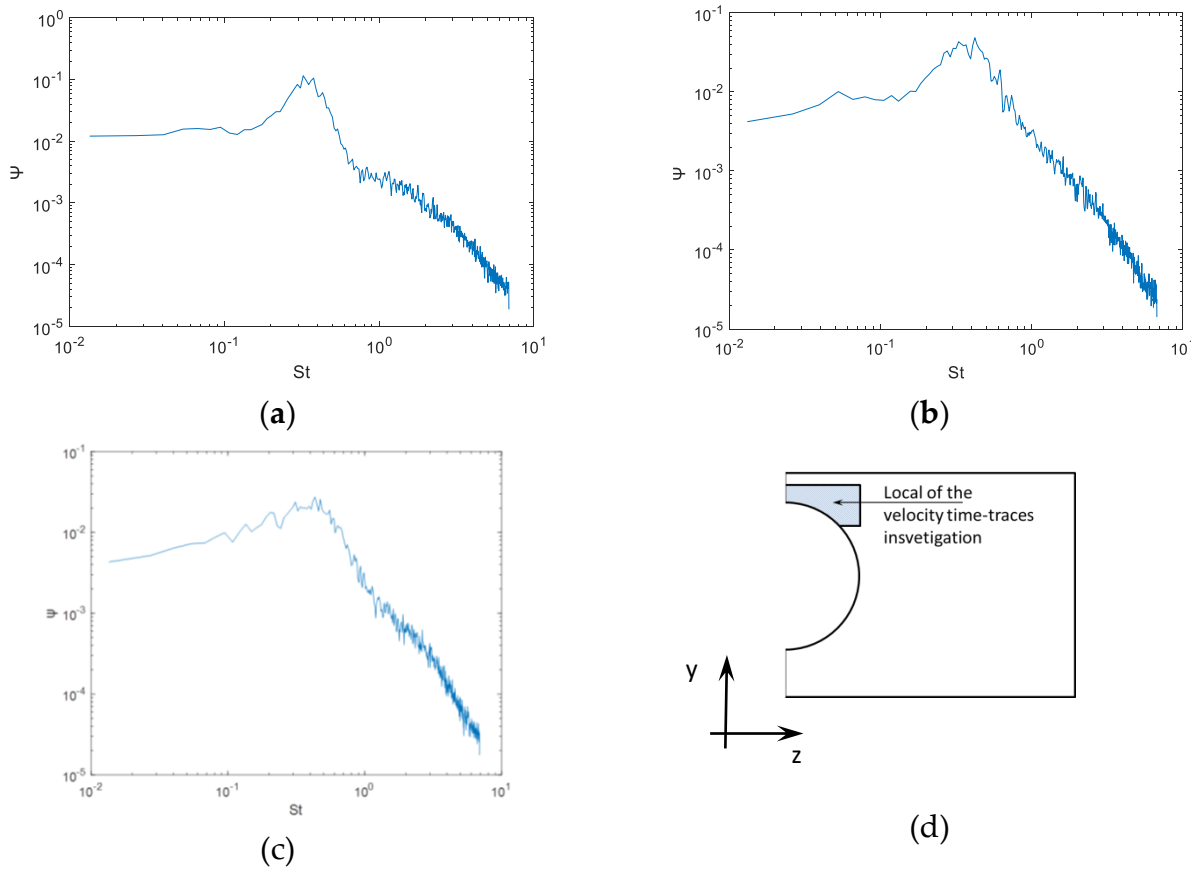

Figure 6. Dimensionaless spectra of the fluctuating axial velocity. (**a**) *W/D* = 1.05; (**b**) *W/D* = 1.10; (c) W/D = 1.15; (d) locus of the velocity time-traces collection.

4. Conclusions

In this work, it was assessed experimentally the influence of the turbulent flow and gap spacing in the wall temperature distribution around the rod and the local Nusselt number as well. The experiments were carried out in a

rectangular channel containing a single rod bundle in the core. Local wall temperature was measured by using a heat cell completely designed and built in our laboratory. The velocity time-traces were also gathered and analyzed for all three gap spaces, W/D = 1.05, 1.10 and 1.15.

The temperature distributions for W/D = 1.05, 1.10 and 1.15 showed the lowest values, and therefore, the highest $h_\phi / \overline{h}$ ratio, in the wider region of the channel. Near the narrow, the temperatures were seen higher than other points, as already expected. A slight difference in terms of temperature was observed as the gap become wider, yielding a temperature decrease in the region. For both, the W/D =1.05 and 1.10, maxima temperature did not occur right just in the narrow gap, but nearby. This finding might be connected to the large-scale structures that dominate the flow in the gap, transferring mass and energy, through the narrow gap, from one subchannel to another. Being the narrow gap dominated by such structures the wall temperature is no longer ruled exclusively by local Reynolds and Prandlt, actually, the local convective heat transfer in the narrow gap might be affected by the presence of the large vortices enhancing the heat transfer process, ending up in the rod wall cooling. Finally, the J-data as function of the gap spacing, W/D, was computed along with results from other researchers. The results from our experimental campaign were found in very fair agreement with those previously stressed in 70's and 90's. J-data was found to approximate one as the gap space increases, as expected.

The spectra for W/D = 1.05, 1.10 and 1.15 showed very pronounced peaks with a fundamental dimensionless frequency. To scale the frequency the Strouhal number was computed as follow in the previous research (Guellouz and Tavoularis, 2000; Severino , 2018; Chang and Tavoularis, 2007 and 2007).

The high level of the energy was found in the Strouhal number 0.42 for both wider gaps (W/D = 1.10 and 1.15), whereas for the narrowest one it was identified at St = 0.33. These values are twice, at least, from the values found by other researcher who published such number about 0.20. The difference may be attributed to the rod itself. In the previous cases the rod is hollow and in our case the rod is closed in both ends. Such slighted difference affects the local Reynolds since the mass is redistributed in different way in both configurations.

Acknowledgments: Fábio Matos Kayser would like to thank the Coordenação de Aperfeiçoamento de Pessoal de Nível Superior – Brasil (CAPES) – Finance Code 001 and FAPDF through the research project nº 0193.001.356/2016 (FAPDF) for supporting me during this research. Jalusa Ferrari thanks to FAPDF for supporting them with fellowships during the work through the research project n° 0193.001.356/2016. Jhon Nero Vaz Goulart would like to thank to CNPQ and FAPDF for supporting him with a financial aid through the research projects nº 408869/2016-0 (CNPQ), 0193.001.158/2015 (FAPDF) and 0193.001.356/2016 (FAPDF).

References

1. Goulart, J.N.V.; Wissink, J.G.; Wrobel, L.C. (2016). Numerical of turbulent flow in a channel small slot. Int. Journal of Heat and Fluid Flow, pp. 343–354.
2. Melo, T.; Goulart, J. N. V.; Anflor, C. T. & Santos, E. (2017). Experimental investigation of the velocity time-traces of the turbulent flow in a rectangular channel with a lateral slot. European Journal of Mechanics-B/Fluids, Vol. 62, pp. 130–138.
3. Severino, H. A. M.; Melo, T. & Goulart, J. N. V. Hot wire anemometry and numerical simulation applied to the investigation fo the turbulence in a gap flow. 6th European Conference on Computational Mechanics (ECCM 6) and 7th European Conference on Computational Fluid Dynamics (ECFD 7) - ECCOMAS 2018. Glasgow, UK.
4. Candela, D.S.; Gomes, T.F. & Goulart, J.N.V. (2020). Numeric simulation of turbulent flow in an eccentric channel. European Journal of Mechanics / B Fluids, Vol. 83, pp. 86–98.
5. Palmer, L. D. & Swanson, L. L. (1961). Measurements of heat-transfer coefficients, friction factors, and velocity profiles for air flowing parallel to closely spaced rods (No. GA-1787). General Dynamics Corp., San Diego, CA (United States). General Atomic Div.
6. Groeneveld, D.C. (1973). Forced convective heat transfer to superheated stem in rod bundles, AECL Report, AECL-4450, Chalk River, Ontario. Canada.
7. Ouma B.H. & Tavoularis. S. (1991). Turbulence structure in triangular subchannels of a reactor bundle model. Nucl Eng Des., 128, p 27 1-287.
8. Guellouz, M.S. & Tavoularis S. (1992). Heat transfer in rod bundle subchannels with varying rod-wall proximity. Nuclear Engineering and Design, pp. 351–366.
9. Makhmalbaf, M. H. M. (2012). Experimental study on convective heat transfer coefficient around a vertical hexagonal rod bundle. Heat and mass transfer, Vol 48, n. 6, pp. 1023-1029.

10. Tavoularis, S., & Chang, D. (2007, July). Inter-subchannel Mixing across very Narrow Gaps in Rod-bundles. In 15th International Conference on Nuclear Engineering (pp. 22-26).
11. Chang, D., & Tavoularis, S. (2008). Simulations of turbulence, heat transfer and mixing across narrow gaps between rod-bundle subchannels. Nuclear Engineering and Design, 238(1), 109-123.
12. Guellouz, M. S. (1998). Turbulent flow and heat transfer in rod bundles. Ph.D. thesis, University of Ottawa, Ottawa, Canada.
13. Hofmann, G. (1964). Qualitative investigation of local heat transfer coefficients in a 7-rod bundle. In Report No. 13. Institut für Reaktorbauelemente KfK Karlsruhe FRG.Rowe, D. S. (1973). Measurement of turbulent velocity, intensity and scale in rod bundle flow channels.
14. Hooper, J. D., & Rehme, K. (1984). Large-scale structural effects in developed turbulent flow through closely-spaced rod arrays. Journal of Fluid Mechanics, 145, 305-337.
15. Möller, S. V. (1991). On phenomena of turbulent flow through rod bundles. Experimental thermal and fluid science, 4(1), 25-35.
16. Meyer, L., & Rehme, K. (1994). Large-scale turbulence phenomena in compound rectangular channels. Experimental Thermal and Fluid Science, 8(4), 286-304.
17. Meyer, L., and Rehme, K. (1995). Periodic vortices in flow through channels with longitudinal slots or fins. In 10th Symposium on Turbulent Shear Flows, the Pennsylvania State University, University Park (pp. 14-16).
18. Meyer, L. (2010). From discovery to recognition of periodic large scale vortices in rod bundles as source of natural mixing between subchannels—a review. Nuclear Engineering and Design, 240(6), 1575-1588.
19. Guellouz, M.S. & Tavoularis, S. (2000). The structure of the turbulent flow in a rectangular channel containing a single rod-Part 1: Reynolds-Average measurements. Exp Thermal and Fluid Science, Vol. 23, pp. 59-73.
20. Ferrari, J. M. da S., & Goulart, J. N. V. (2016). Simulação Numérica do Escoamento Laminar em um Canal Complexo. Revista Interdisciplinar De Pesquisa Em Engenharia, 1(2). https://doi.org/10.26512/ripe.v1i2.14435